Fabrication and Characterization of Composites of a Perovskite and Polymers with High Dielectric Permittivity

S. Bahar Basturk, Claire E.J. Dancer, Tony McNally

PII: S0025-5408(20)31607-X

DOI: https://doi.org/10.1016/j.materresbull.2020.111126

Reference: MRB 111126

To appear in: *Materials Research Bulletin*

Received Date: 12 June 2020

Revised Date: 16 October 2020

Accepted Date: 8 November 2020

Please cite this article as: Basturk SB, Dancer CEJ, McNally T, Fabrication and Characterization of Composites of a Perovskite and Polymers with High Dielectric Permittivity, *Materials Research Bulletin* (2020), doi: https://doi.org/10.1016/j.materresbull.2020.111126

Fabrication and Characterization of Composites of a Perovskite and Polymers with High Dielectric Permittivity

S. Bahar Basturk[1,2]*, Claire E.J. Dancer[2], Tony McNally[2]

[1]Department of Metallurgy and Materials Engineering, Manisa Celal Bayar University, Turkey

[2]Internationational Institute for Nanocomposite Manufacturing (IINM), WMG, University of Warwick, CV4 7AL, UK.

Corresponding Author: S. Bahar Basturk, e-mail: bahar.basturk@cbu.edu.tr

Graphical abstract

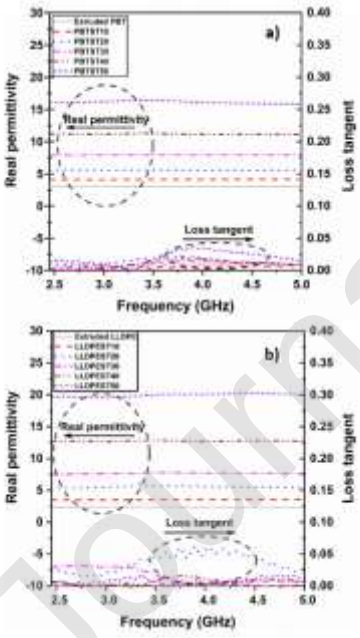

Highlights

- Composites of $SrTiO_3$ with PBT and LLDPE were readily prepared by extrusion
- $SrTiO_3$ volume loadings as high as 50% achieved
- $SrTiO_3$ has a nucleating effect on both polymers, reducing crystalline content
- The dielectric permittivity (ε') of PBT increased from 3.7 to 16.5
- ε' of LLDPE increased from 2.3 to 19.7
- Good agreement between the Lichtenecker model and experimental values of ε'

Abstract

Composites of strontium titanate ($SrTiO_3$) at loadings up to 50vol.% with polar poly(butylene terephthalate) (PBT) and non-polar linear low density polyethylene (LLDPE) were prepared **to investigate their dielectric responses in wireless frequency range**. The $SrTiO_3$ particles were uniformly dispersed in polymers at low loadings, but were more bead-like and agglomerated at higher $SrTiO_3$ loadings. The $SrTiO_3$ has strong nucleating effect on both polymers, increasing the crystallization and reducing the crystallinity of both polymers. Dielectric properties of composites were measured between 2.45-5 GHz. Dielectric permittivity (ε') of composites at 2.45 GHz increased with increasing $SrTiO_3$ content. ε' increased by a factor of 5 for PBT, from 3.7 for unfilled PBT to 16.5 and by a factor of ~8.5 for unfilled LLDPE, from 2.3 to 19.7 for maximum $SrTiO_3$ loading. The composites had similar dissipation factor values as the unfilled polymers. **The Lichtenecker model was in good agreement with the experimental data.**

Keywords: Strontium titanate ($SrTiO_3$); Polymer composites; Dielectric properties; Permittivity; Microwave frequency

1. Introduction

Microwave characteristics of materials, particularly when used at high operating frequencies in electronic applicances like computers and smart phones are critically important. Dielectric materials are one of the most attractive candidates for such applications due to their high dielectric permittivities (real part permittivity-ε'), low dissipation factor (loss tangent-$tan\delta$) as well as improved energy storage capacity and are utilized in many applications such as antennas, microwave absorbers, waveguides, sensors and capacitors [1-3].

Conventionally, titanate (TiO_2), barium titanate ($BaTiO_3$, BT) barium strontium titanate ($BaSrTiO_3$, BST), lead zirconate titanate (PZT), magnesium oxide (MgO), barium zirconate titanate (BZT) ceramics and metal phenylphosphonates are commonly preferred due to their promising electrical properties [4]. Perovskite type ceramics (general stoichiometry of ABO_3) show unique crystalline structures that leads to superior dielectric properties. Strontium titanate ($SrTiO_3$) is a member of the perovskite group of material and has mixed ionic-covalent bonding properties [5]**. Barium titanate is the mostly studied perovskite as a potential capacitor material/component. However, with 7-10 times higher permittivity, relatively better thermal stability, higher break down strength and lower dissipation factor values of $SrTiO_3$ has captured the attention of researchers [5-6].**

While having remarkable optical, dielectric and thermal properties, perovskite synthesis requires high sintering temperatures **as for other ceramics [7]**. **In various studies $SrTiO_3$ is modified by introducing different components such as glass or**

ceramic compounds to obtain exceptional properties for different applications [5]. For instance, Naidu et al. examined the dielectric effects of MgO doped $SrTiO_3$ ceramic in the 0.1 kHz to 5 MHz frequency range [8]. The dielectric permittivity and loss tangent values were determined as 45.43 and 0.162 at 5 MHz, respectively. Yang et al. investigated the $SrTiO_3$-BNT-BLZT lead free ceramic films and based on their study the increase of BNT-BLZT content led to an increase in ε' (~4000) and $tan\delta$ (~0.15) at 1 MHz and room temperature [9]. Polycrystalline bismuth and lithium co-substituted strontium titanate $Sr(1-x)(Bi,Li)xTiO_3$ was prepared via a solid-state method by Alkathy and Raju [6]. At 25°C and 1 kHz when x=0.8, the dielectric permittivity was enhanced from 246 to 1173 while the loss tangent was 0.0167. As given in the examples above, many studies in the literature explore the doping effects of various elements and achieve interesting results. However, their manufacturing routes are relatively complicated and mass production is limited.

Polymer based composites made of nano-size fillers generally show outstanding properties due to the unique features of nanoparticles such as high surface to volume ratio and large interfacial area forming between matrix and nanoparticle. The interface between the (nano)composite components govern the increases in mechanical, electrical and thermal properties [10]. Moreover, for electric/electronic and energy storage/conversion applications, nanocomposites have potential in aerospace, biochemistry, automative and packaging industries [11,12]. (Nano)composites combining the advantages of polymer and filler (ceramic) can be processed easier and are viable alternatives to single/**doped** ceramic materials [2].

Composites of polymers and perovskites have been prepared previously to form structures with high dielectric permittivity and low loss tangent. The dielectic performance of composites of polymers and perovskites is determined from several parameters such as filler volume fraction, particle size and shape as well as the level of dispersion and distribution in the polymer matrix [13].

Lee at el. compared the dielectric performance of $BaTiO_3$/epoxy and $SrTiO_3$/epoxy composite films between 2-10 GHz. For the same volume fractions (50 vol.%) at 5 GHz, $SrTiO_3$ based composites had a ε' =~20 and maintained stability over all the frequency range. However, $BaTiO_3$ based samples had ε' =25 which suddenly decreased above 5 GHz [14]. Composites of isophthalic polyester (IP) resin/styrene and nano-$SrTiO_3$ were prepared by Khutia et al. and analysed at 150°C and 10 Hz. The nanocomposite films displayed maximum permittivity as 20 for 20 wt.% particle loading [15]. Nisa et al. studied filler particle size on the dielectric properties of PEEK/$SrTiO_3$ composites with constant 27 wt.% filler content at 1 MHz. The composites produced with nano-size $SrTiO_3$ exhibited higher ε' values whereas the $tan\delta$ values were 10 times higher than the corresponding composites produced with micro-size particles [16].

Although there have been a **relatively** small number of studies on the electrical/dielectrical properties of $SrTiO_3$ based composites, there has been limited research on the dielectric properites of composites of $SrTiO_3$ filled thermoplastics at high frequencies (>1 MHz). **Rajesh and his co-workers concentrated on the dilectric properties of PTFE/$SrTiO_3$ composites between 1 kHz-40 MHz and reported that a 60**

wt.% loaded polymer displayed the highest ε' (~11) [17]. Thomas *et al.* studied the dielectric characteristics of composites of butyl-rubber and $SrTiO_3$ at 1 MHz and 5 GHz as a function of $SrTiO_3$ concentration, in the range 10% to 40% by volume. They showed that the composite sample with 0.42 volume fraction $SrTiO_3$ exhibited ε' and $tan\delta$ values of 13.2 and 2.8×10^{-3} at 5 GHz [18]. Likewise, Xiang et al. demonstrated that the introduction of 40 volume percent $SrTiO_3$ into a polyoxyethyelene (POE) matrix resulted in an increase in the dielectric constant from ε_r=2.1 (for pure POE polymer) to ε_r=11 with $tan\delta$=0.01 at 5 GHz [19].

Polybutylene terephthalate (PBT) is a polar thermoplastic and particularly used in electrics/electronics and automative industry while linear low density polyethylene (LLDPE) is a widely known non-polar polymer with low cost and can be utilized in similar types of applications [20-21]. The chemical structures of linear LLDPE and PBT are given in Figure S1 (Supplementary Information).

In this work, hybrid composites of either polar polybutylene terephthalate (PBT) or non-polar linear low density polyethylene (LLDPE) and nano-sized $SrTiO_3$ at loadings up to 50 vol%. were prepared by melt compounding in a twin-screw extruder. In contrast with the majority of studies, the composites were prepared using a scalable and continuous extrusion process. The dispersion and distribution of the $SrTiO_3$ particles in the polymer matrices were examined and the crystalline and thermal characteristics of the composites determined using a range of techniques. The dielectric properties of the composites were measured between 2.45-5 GHz (microwave frequencies) using a vector network analyzer (VNA) to study composite responses in the wireless frequency (**WiFi**) range. **For an**

ideal/optimum capacitor material used in telecommunication applications, an increase in dielectric permittivity and reduction of dissipation factor are required. In the present work, composites of PBT and LLDPE with $SrTiO_3$ were prepared by extrusion and their dielectric properties were studied as a function of filler loading. Additionally, a number of analytical models were used to predict the dielectric permitivitty of the composites and the values obtained compared with those measured experimentally. **Among the models applied, Lichtenecker's approach provided the best convergence and matched very well with the experimental results.**

2. Experimental Section

2.1. Materials

Strontium titanate ($SrTiO_3$) perovskite powder with a 600-800 nm average particle size (density 4.70 g/cm^3 and 2060°C melting temperature) was purchased from TPL™, USA. The $SrTiO_3$ had a 100% cubic structure, see X-ray diffractograms in Figure S2. Pocan B polybutylene terephthalate (PBT) pellets, density of 1.3 g/cm^3 density and melting temperature, T_m=225°C was purchased from Lanxess™, Germany and dried as per the manufacturers guidelines before use. The linear low density polyethylene (LLDPE), density =0.9 g/cm^3 and T_m=120-125°C was supplied by Terplast™, Italy.

2.2. Fabrication of Composites

Composites of PBT and LLDPE with $SrTiO_3$ at loadings of 10vol.%, 20vol.%, 30vol.%, 40vol.% and 50vol.% were prepared and the following composite nomenclature adopted

depending on polymer type and filler volume fraction, e.g. PBTST20 is 20vol.% $SrTiO_3$ in PBT or LLDPEST50 is 50vol.% $SrTiO_3$ in LLDPE. In the first instance, the as-received granulated polymers were placed into a special vial and cryo-milled in a liquid N_2 environment using a Freezer Mill (SPEX™) and converted to a powder. The $SrTiO_3$ particles were then dry mixed with the PBT or LLDPE powders manually in the desired ratios. The dry blend mixes were then mixed using a mechanical mixer before extrusion. The PBTST was extruded applying a temperature profile of 215°C-250°C using a co-rotating 24 mm twin screw extruder (Thermo Scientific, TSE 24 MC). The LLDPEST were compounded with the same machine but with a temperature profile of 135°C-145°C along the extruder barrel. In both instances, a screw speed of 40 rpm was employed and the resultant composite materials were cooled in a water bath before pelletising.

2.3. Characterization

The morphology of the composites and the extent of the distribution of the $SrTiO_3$ particles in the polymer matrices were investigated using a Carl Zeiss™ Sigma Field Emission Gun–Scanning Electron Microscope (FEG-SEM) under an accelerating voltage between 2-10 kV with a back scattering electron (BSE) detector. Composite samples were sputter coated with Au prior to imaging.The thermal properties of neat polymers and all composites were studied using Differential Scanning Calorimetry (DSC) using a Mettler Toledo DSC instrument in air and a heating rate of 10 K/min. In the first stage of the DSC measurements, all the specimens were kept at a maximum temperature for 5 minutes to

remove the thermal history due to extrusion. The degree of crystallization was determined from:

$$X_c = \frac{\Delta H_m}{\Delta H_m^0 (1 - X_f)} \times 100 \qquad (\mathbf{1})$$

where,X_f, ΔH_m and ΔH_m^0 are weight fraction of filler, the melting enthalpy of the sample and for a theoretically 100% crystalline polymer ΔH_m^0 for PBT and LLDPE were taken as 140 J/g and 290 J/g, respectively [22-23]. In order to determine the dielectric properties of the composites in the 2.45-5 GHz frequency range, a two-port Vector Network Analyzer (VNA, Keysight Agilent N1500A) was used via transmission line and free space method and co-axial probe measurement. The dielectric specimens with 7 mm cylindirical geometry were prepared with a bespoke hot pressing technique at 10 bar pressure using a mould and cut to precise dimensions. The PBTST and LLDPEST composites were pressed at 230°C and 145°C, respectively. The Nicolson-Ross-Weir model was used to estimate the dielectric properties, including real dielectric permittivity (ε') and loss tangent ($tan\delta$) [24]. Fourier transform infrared spectroscopy, X-ray diffraction and thermogravimetric analysis was also performed on all materials and the experimental detail is given in Supplemenatary Information.

3. Results and Discussions

3.1. Morphological Characterization

The morphology and extent of $SrTiO_3$ dispersion as a function of loading (by volume) in PBT was examined and imaged by SEM, see Figure 1(a)-(f). Firstly in Figure 1 (a), the as-received nano-$SrTiO_3$ particles tended to be agglomerated from 600nm up to a

few microns in size. Unsurprisingly, with increasing $SrTiO_3$ loading the number of $SrTiO_3$ agglomerates increased, Figure 1 (b) to (f). Indeed, up to theoretical loadings of 40vol.% and 50vol.% the $SrTiO_3$ particles homogeneously cover the surface of the PBT. At higher magnification (see images inset in Figure), some cavities can be observed which can be attributed to the $SrTiO_3$ particles being pulled out of the PBT matrix during fracturing and the limited wetting between $SrTiO_3$ particles and PBT. The extent of $SrTiO_3$ dispersion in LLDPE was also investigated by SEM, see Figure 2. From Figures 2 (a) and (b), the LLDPEST composites with theoretically 10vol.% and 20vol.% $SrTiO_3$ exhibited more striated 'fibral-like' structures and micropores on the polymer surface. The $SrTiO_3$ particles appear to be preferentially located between these structures which can be seen more clearly at higher magnifications, see inset Figures. There appears to less agglomeration of the $SrTiO_3$ when mixied with LLDPE. With increasing $SrTiO_3$ content, particularly in the case of the LLDPEST40 and LLDPEST50 composites, it appears that the particles are embedded more uniformly in the LLDPE matrix. High shear forces applied during extrusion breaks down the harsh agglomerates and a relatively homogeneous distribution of $SrTiO_3$ particles was obtained. **The agglomeration of ceramic particles can be hindered by applying surface modification techniques such as silane coupling treatment** [**4, 11, 25**].

The FTIR spectra of the composites suggest there are no clear interactions between $SrTiO_3$ and either polymer, see Figure S3.

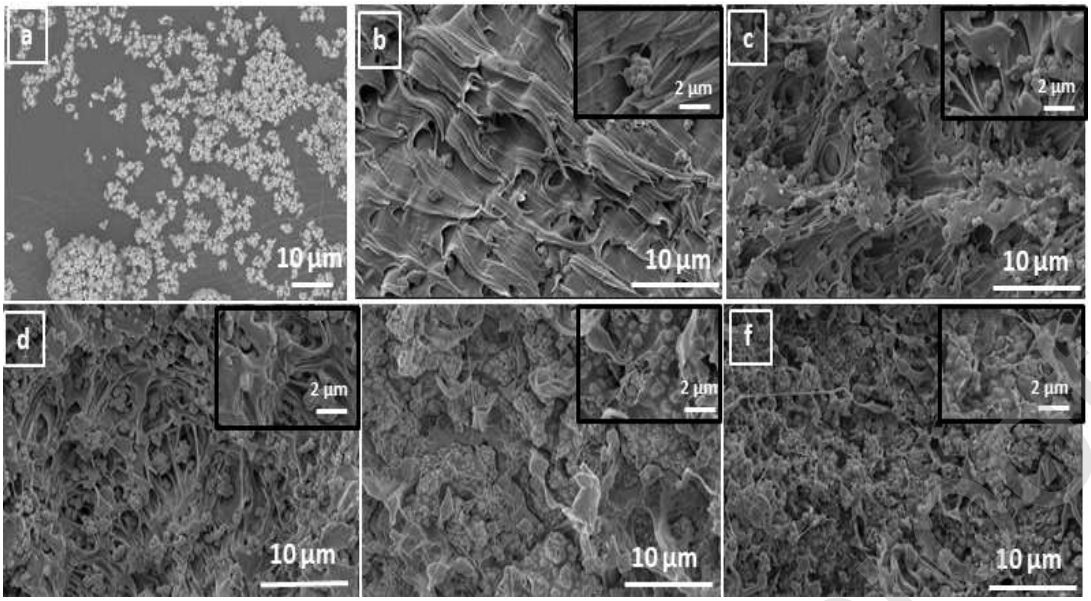

Figure 1. SEM micrographs of a) as-received $SrTiO_3$ powder and b) PBTST10, c) PBTST20, d) PBTST30, e) PBTST40 and f) PBTST50 composites. Inset images are taken at higher magnification.

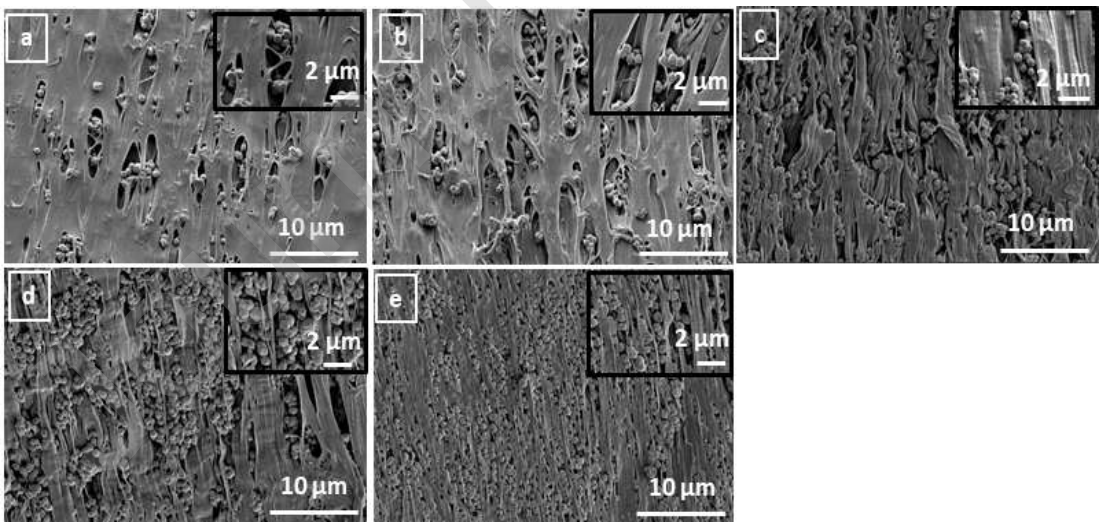

Figure 2. SEM micrographs of a) LLDPEST10, b) LLDPEST20, c) LDPEST30, d) LDPEST40 and e) LDPEST50 composites.

3.2. Thermal Properties

The thermal properties of $SrTiO_3$ and all composites were studied using DSC (Figure 3) and TGA (Figure S4 and Table S1). Figure 3 (a) and (b) show the cooling and heating curves of PBTST composites obtained from the first cooling and second heating cycles, respectively, from which the following parameters were determined, melting temperature (T_m), crystallization temperature (T_c), crystallization enthalpy (H_c), melting enthalpy (H_m) and degree of cristallinity ($X_c\%$), and are listed in Table 1. Inclusion of $SrTiO_3$ to PBT resulted in an increase in T_c by ~8°C, from ~192°C for neat PBT to ~200°C for the composite with 10vol% $SrTiO_3$ before decreasing to 196°C for the 50vol% composite but still higher than PBT itself. There was no significant change in T_m of the composites relative to unfilled PBT, but all composites displayed a doublet of melting peaks, which is related to the process of melting-recrystallization-remelting. The presence of this doublet of endothermic peaks is derived from the different PBT crystal structures, size and packing perfections as well as the variation in crystallite thicknesses [22,30]. The PBT crystallinity ($X_c\%$) decreased significantly with increasing addition of $SrTiO_3$. For PBT, post extrusion, $X_c\%$ = 44.2% but for the PBTST50 composite $X_c\%$=12.1%. The addition of such a large volume of $SrTiO_3$ to the PBT matrix significantly retards polymer chain mobility and hindering PBT crystallization [20,31].

Similar behaviour in T_c was obtained for the LLDPEST composites, Figure 3 (c) and (d), in that T_c of LLDPE increased with increasing $SrTiO_3$ content by ~5°C from ~105°C for unfilled LLDPE to ~110°C for the composite with 50vol.% $SrTiO_3$. As was the case for PBT, the T_m of LLDPE was unchanged irrespective of the $SrTiO_3$ loading. Again, $X_c\%$ decreased with increasing $SrTiO_3$ content, from 33.2% for unfilled LLDPE to 21.8% for LLDPEST50, see Table 1. The reduction in LLDPE crystallinity can again be related with the confinement of polymer chains by the $SrTiO_3$ particles with increasing volume fractions [32]. Increasing addition of filler prevents the molecular movement of chains into the crystal lattice and resulting in a decrease in $X_c\%$, as in this work [33-34].

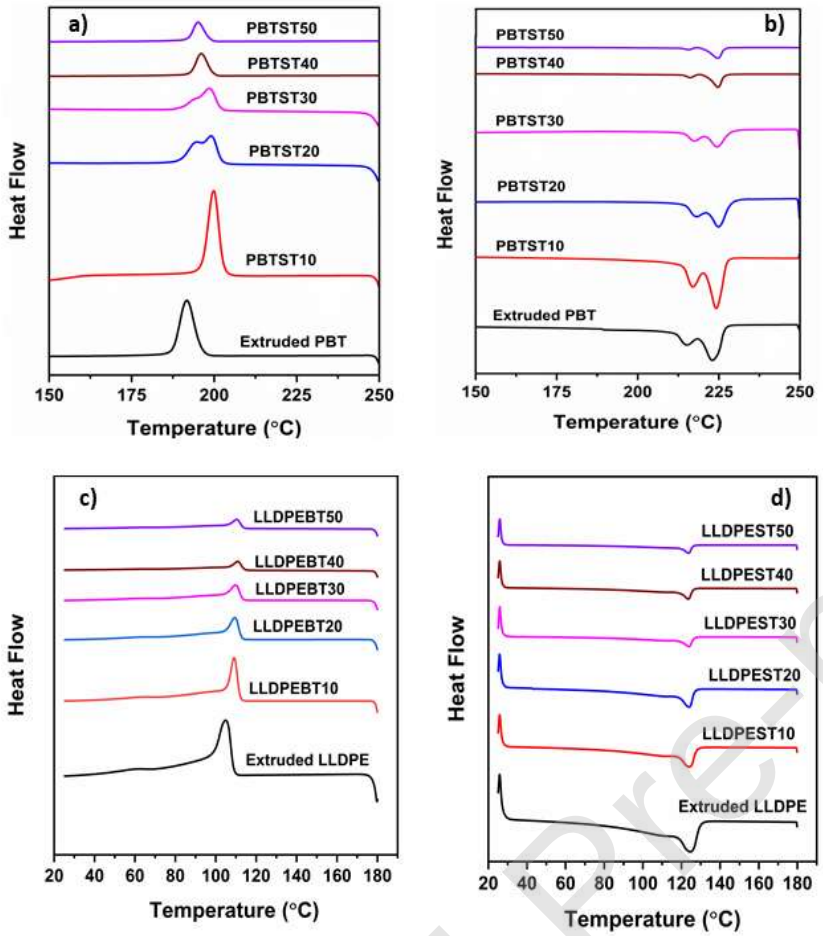

Figure 3. DSC curves showing a) crystallization exotherms and b) melting endotherms of extruded PBT and PBTST composites, c) crystallization exotherms and d) melting endotherms of extruded LLDPE and LLDPEST composites

Table 1. Thermal parameters for composites of $SrTiO_3$ with PBT and LLDPE, from DSC measurements.

Material	T_m (℃)	ΔH_m (j/g)	T_c (℃)	ΔH_c (j/g)	X_c%
PBT	222.7	61.9	192.1	35.9	44.2
PBTST10	223.7	48.7	200.6	50.9	40.8
PBTST20	224.7	28.8	199.2	27.2	28.5
PBTST30	224.3	15.2	198.6	18.1	19.3
PBTST40	223.4	6.7	197.7	7.9	13
PBTST50	223.3	6	196	6.3	12.1
LLDPE	124.2	96	105.3	100.7	33.1
LLDPEST10	124	64.4	107.1	64.5	31.5
LLDPEST20	123.6	42.5	107.9	44.7	24.8
LLDPEST30	123.7	26.7	108.3	28.8	23.7
LLDPEST40	123.4	23.1	108.4	28.1	24.1
LLDPEST50	123.6	16	110.1	15.1	21.8

3.3 Dielectric Properties

In an applied electric field, polarization occurs and leads to the enhancement of charge storage ability of dielectric materials. This ability is represented by complex permittivity, ε^* and can be exhibited in the frequency domain as in Eq. (2). In this formula, ε^* corresponds

to the complex permittivity while ε' and ε'' describe the real part of permittivity (i.e. dielectric permitivitty) and imaginary part permittivity (i.e loss factor or dielectric loss factor), respectively [**36**].

$$\varepsilon^* = \varepsilon' - j\varepsilon'' \quad (2)$$

The dissipation factor (loss tangent) is a measure of energy loss in the dielectric during AC operation, expressed as $tan\delta$ and can be formulated by Eq. (3) [**37**].

$$tan\delta = \frac{\varepsilon''}{\varepsilon'} \quad (3)$$

In this study, the variation in the dielectric constant as a function of frequency was investigated between 2.45 and 5 GHz to reveal the dielectric characteristics of $SrTiO_3$ based polymer composites. This frequency range was selected to accurately understand the performance of the composites with different filler concentrations for wireless communication applications. Both dielectric (real) permitivitty and the loss tangent values were specified by considering the measured S-parameters based on the Nicolson-Ross-Weir (NRS) approach by utilizing VNA. A co-axial probe method was used to characterize the dielectric properties since the measurements are relatively simple to do. ε' for PBT, LLDPE and $SrTiO_3$ was measured to be 3.7, 2.3 and 300, respectively [**38-39,7**]. Figure 4 (a) and (b) shows the variation in ε' and ε'' for PBTST and LLDPEST as a function of frequency. It is known that ceramic perovskite particles contribute to the increase in permitivitty of polymer based composites due to their high polarity [**40-41**]. Here, ε' for neat PBT increased from 3.7 to 16.5 on inclusion of 50vol.% $SrTiO_3$ (0.35 actual volume fraction) at 2.45 GHz. Similarly, ε' of LLDPE increased from 2.3 to 19.7 for addition of 50vol.%

$SrTiO_3$ (actual volume fraction 0.46) at 2.45 GHz. The permitivitty values remain almost constant and independent of frequency.

Under an electrical field, a dielectric material displays one of four types of polarization mechanisms: electronic, ionic, dipole and interfacial (Maxwell-Wagner-Sillars,MWS) polarization. The structure of the material and frequency range govern the polarization characteristics. In hybrid materials/**heterogeneous systems**, interfacial polarization (Maxwell-Wagner-**Sillars or space charge polarization**) is the dominant mechanism, **particularly** at low frequencies [**4,25**]. **If one of the components of a composite is conductive, space charge polarization is also observed even at microwave frequencies (300 MHz-300 GHz) [42-43].**

In our study, the presence of mini-capacitors with high dielectric permitivitty (i.e. the $SrTiO_3$) [**44**] in the composites and the atomic polarization effect [24] give rise to the improved permittivity at **the high frequency band**. The increase to high filler loadings, results in an increase in ε', which can be related to the finer dispersion of $SrTiO_3$ particles in the composite microstructures [**44**]. The variation in $tan\delta$ with frequency is also shown in Figure 4. Independent of polymer type, no consistent relationship was observed between $SrTiO_3$ content and loss tangent values of the composites. Unfilled PBT and LLDPE had $tan\delta$ values of 0.0083 and 0.0003, which changed little during measurement, **particularly for lower filler loading**. At 5 GHz, the composites exhibited similar $tan\delta$ values close to that of the neat polymer. However, the $tan\delta$ values for the LLDPE composites were generally higher than the unfilled LLDPE at the same frequency.

One of the major motivations for this study was to compare the dielectric performance of composites of $SrTiO_3$ with a polar polymer (PBT) and non-polar polymer (LLDPE). From experimental TGA and density measurements (Archimedes), see Figure S4 and Table S1 the actual $SrTiO_3$ content in the composites did not fit with the theoretical volume fractions. However, composites with similar actual filler loading, e.g. PBTST30 and LLDPEST20, the values of ε' were 7.87 and 5.25, respectively. Likewise, for PBTST50 and LLDPEST40 (i.e. with very similiar actual $SrTiO_3$ content - 36.3-36.7 vol.%) ε' was 16.05 and 12.75, respectively. Therefore, composites of $SrTiO_3$ with the more polar PBT yield higher ε' values. **Table 2 lists the dielectric properties of various filler/polymer matrix composites with different particle size and concentration. It is known that several parameters such as production conditions, particle distribution, polymer properties, filler concentration and frequency have major affects on dielectric response of composites. It is clearly seen from Table 2 that the composites below 10 MHz generally had higher values depending on filler content and grain size. Based on the literature, in the high frequency domain the dipoles do not have sufficient time to align with the applied electrical field and this results in a reduction in permittivity [45]. Therefore, it is probable that the composites described in this study should achieve improved permittivities at lower frequeny band. From Table 2, the silicon rubber/$BaTiO_3$ composite exhibited favorable ε' at 5 GHz. However, the $tan\delta$ value of this composite was relatively high when compared to those described in this work [46]. The dielectric performance of $BaTiO_3$/epoxy composites with two different filler sizes (100 mm and 200 nm) were given in the same table. Although ε' of these latter**

samples displayed similar values with the LLDPEST composites in this study (for similar volume fractions), their loss tangent values were pretty high at 5 GHz. The PBTST composite showed better dielectric permittivity and *tanδ* when compared to [45] at the same frequency. In comparison with $BaTiO_3$ counterparts, $SrTiO_3$ based composites generally show lower loss tangent values (below 0.02) [5], further evidence for an ideal capacitor material, as seen in Table 2.

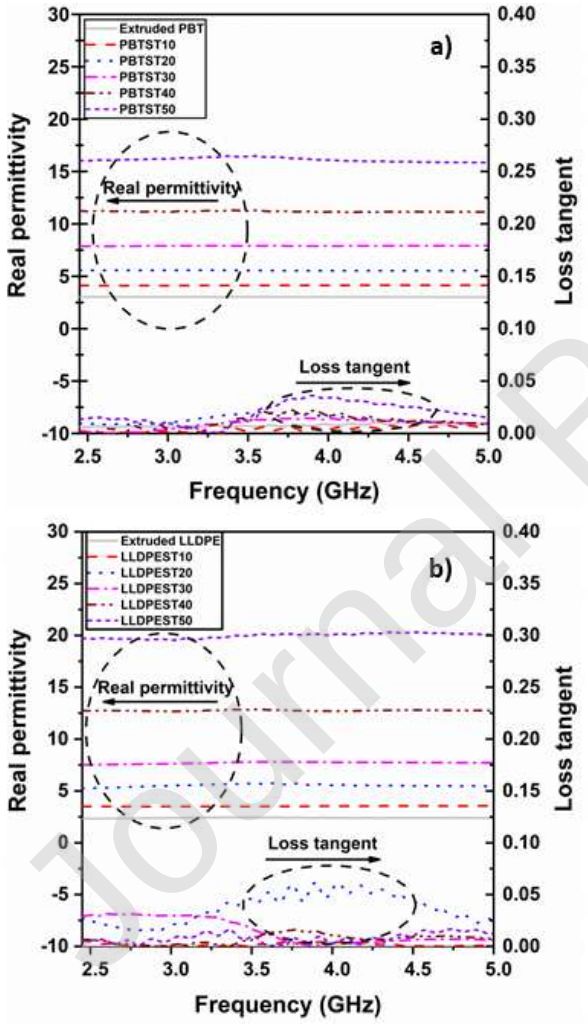

Figure 4. Variation in real permitivitty (ε') and loss tangent (*tanδ*) for composites of $SrTiO_3$ with a) PBT b) LLDPE.

Table 2. Comparison of the dielectric properties of composites of $SrTiO_3$ or $BaTiO_3$ with different polymers

Filler	Filler loading & size	Matrix	ε'	*tan* δ	Reference
$BaTiO_3$	40 vol.% (100 nm)	Epoxy	~11 @ 5 GHz	0.05 @5 GHz	**45**
$BaTiO_3$	40 vol.% (200 nm)		~15 @ 5 GHz	0.06 @5 GHz	
$BaTiO_3$	28 vol.% (900 nm)	Silicone rubber	13 @ 5 GHz	~0.04 @ 5 GHz	**46**
$BaTiO_3$	45 vol.% (~1 μm)	Epoxy	34.9 @1 kHz	0.011 @1 kHz	**47**
$SrTiO_3$	50 vol.% (1 μm)		30.2 @1 kHz	0.013 @1 kHz	
$SrTiO_3$ (heat treated)	55 wt.% (100 nm)	Unsaturted polyester	12 @ 10 MHz	0.015 @ 10 MHz	**48**
$BaTiO_3$	60 vol.% (~7 nm)	PVDF-HFP	25 @ 1 MHz	0.12 @ 1 MHz	**49**
$Ba_{0.7}Sr_{0.3}TiO_3$	50 vol.% (300 nm)	PS	10.34 @5 GHz	0.03 @5 GHz	**50**
$SrTiO_3$	36.3 vol% (600-800 nm)	PBT	16 @ 5GHz	0.011 @ 5GHz	This work
	46.7 vol.% (600-800 nm)	LLDPE	20 @5 GHz	0.012 @ 5 GHz	

To precisely determine the dielectric responses of composites, particularly at high frequencies is critical. Several different mathematical models, including, the Lichtenecker, Maxwell-Garnet, Jayasundere, Poon-Shin and Clausius-Mossotti models have been proposed to predict permitivitty [**51-54**] and have been applied here. Figure 5 (a) and (b) compare the experimental dielectric permitivitty values for PBTST and LLDPEST with those determined theoretically for various volume loadings at 2.45 GHz. In all models, "ε_{eff}", "ε_f" and "ε_m" represent the permitivitty of the composite, filler and matrix, respectively and, "f" is the volume fraction of filler.

$$\ln \varepsilon_{eff} = f\ ln(\varepsilon_f) + (1-f)\ln(\varepsilon_m) \quad \text{(Lichtenecker equation)} \quad \textbf{(4)}$$

$$\varepsilon_{eff} = \frac{\varepsilon_m(\varepsilon_f+2\varepsilon_m+2f\varepsilon_f-2f\varepsilon_m)}{\varepsilon_f+2\varepsilon_m-f\varepsilon_f+f\varepsilon_m} \quad \text{(Maxwell-Garnet equation)} \quad \textbf{(5)}$$

$$\varepsilon_{eff} = \frac{\varepsilon_m(1-f)+\varepsilon_f f[3\varepsilon_m/(\varepsilon_f+2\varepsilon_m)]\left[1+\left(3f(\varepsilon_f-\varepsilon_m)/(\varepsilon_f+2\varepsilon_m)\right)\right]}{1-f+f[3\varepsilon_m/(\varepsilon_f+2\varepsilon_m)]\left[1+\left(3f(\varepsilon_f-\varepsilon_m)/(\varepsilon_f+2\varepsilon_m)\right)\right]} \quad \text{(Jayasundere equation)} \quad \textbf{(6)}$$

$$\varepsilon_{eff} = \varepsilon_m\left[1+\frac{f\left((\varepsilon_f/\varepsilon_m)-1\right)}{f+\left(1-\frac{f}{3}\right)\left[\left(\varepsilon_f/\varepsilon_m\right)(1-f)+f+2\right]}\right] \quad \text{(Poon-Shin equation)} \quad \textbf{(7)}$$

$$\varepsilon_{eff} = \varepsilon_m\left[1+3f\left(\frac{(\varepsilon_f-\varepsilon_m)}{(\varepsilon_f+2\varepsilon_m)}\right)\right] \quad \text{(Clausius-Mossotti equation)} \quad \textbf{(8)}$$

The accuracy of the models given above depend on parameters such as the size and shape of the filler powder, microstructural homogenity, porosity, properties of the composite components and interfacial properties [**51**]. As seen in Figure 5 (a), when the $SrTiO_3$ loading is at a minimum in the PBT matrix (~0.05 actual volume fraction), the models and experimental results are in good agreement. However, after this volume fraction, the

Maxwell-Garnet, Clausius Mossotti and Poon-Shin models show siginificant divergence while Lichtenecker and Jayasundere approaches have a better fit with the experimental data. As reported in the literature, Maxwell-Garnet (MG) [**54-55**], Clausius Mossotti (CM) [**56**] and Poon-Shin (PS) [**57**] approaches assume that the spherical dielectric fillers are uniformly dispersed in the continuum medium (polymer phase) without any interactions. For instance, for LLDPEST10 the actual volume fraction of $SrTiO_3$ is 0.09 and Maxwell-Garnet, Clausius Mossotti and Poon-Shin models underestimate the permitivitty. With increasing $SrTiO_3$ loading, this variation becomes more prominent. Therefore these approaches are generally appropriate at lower particle loading. In case of higher loadings, the three models mentioned above can not predict the dielectric permitivitty values of neither PBTST nor LLDPEST composites. The Jayasundere equation is a modified version of Kerner's expression and it takes into account the interactions between neighbouring spherical fillers [**58**]. Although, this model provides better approximations compared to the other models, it shows a divergence at relatively higher $SrTiO_3$ volume fraction (>0.2-0.3) as well. Indeed, Lichtenecker's model describes a binary system composed of randomly oriented uniform spherical shaped particles that show equivalent volumetric distribution [**59**]. In spite of its simplicity, this logarithmic formulation exhibits the best convergence with experiemental data even at high $SrTiO_3$ loadings. Due to the higher actual amount of $SrTiO_3$ in the LLDPE, model results show slight differences in comparison with PBTST counterparts as seen in Figure 5 (b). **In summary, of all the models tested, the Lichtenecker's model matched best with the experimental results for both PBT and LLDPE composites, as seen in Figure 5.**

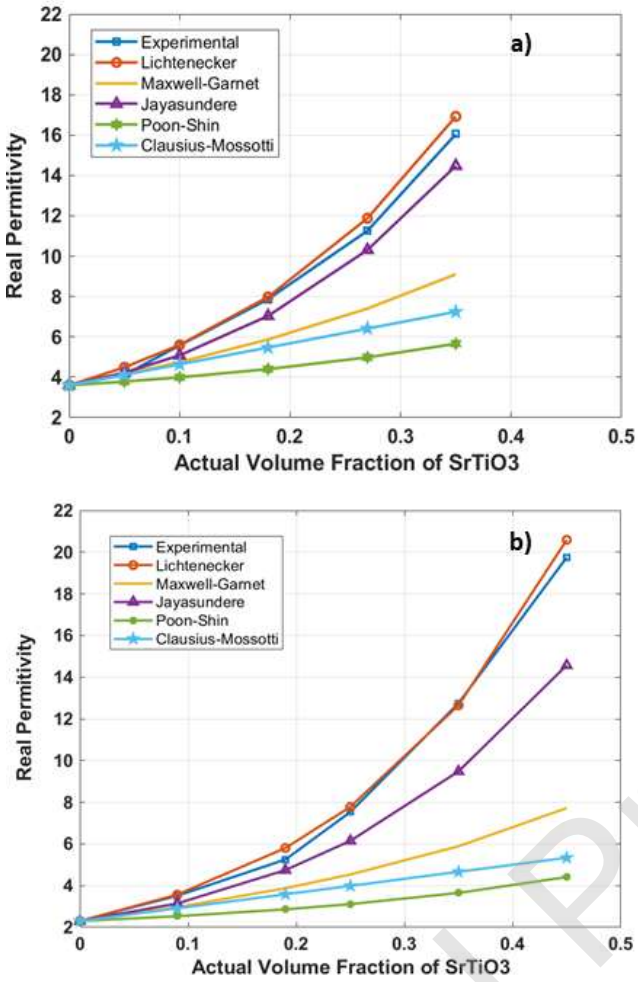

Figure 5. Comparison of dielectric constants determiend experimentally and theoretically for composites of $SrTiO_3$ with a) PBT and b) LLDPE at 2.45 GHz.

4. Conclusions

Composites of $SrTiO_3$ (100% cubic structure) with polar PBT and non-polar linear LDPE were readily produced at ceramic loadings up to 50 vol.% (i.e. 0.5 volume fraction) via melt compounding (extrusion). SEM imaging showed that the $SrTiO_3$ particles were

uniformly dispered and distributed in each polymer matrix. FTIR spectra of the composites suggested there is little interfacial interaction between components. The $SrTiO_3$ particles acted as a nucleation agent for both polymers and increased the crystallization temperature. With increasing $SrTiO_3$ content the crystalline content of both polymers significantly decreased due to major hindering of polymer chain folding. Dielectric measurments in the micorwave frequency range (2.45-5 GHz) revealed that the dielectric (real part) permitivitty (ε') of PBT and LLDPE increased significantly with increasing $SrTiO_3$ volume fraction and that the values of ε' remained almost constant, independent of frequency. ε' increased from 3.7 for unfilled PBT to 16.5 for PBTon addition of 50vol.% $SrTiO_3$ (actual volume fraction 0.35) and for unfilled LLDPE from 2.3 to LLDPEST50 to 19.7 (actual volume fraction 0.46). The $tan\delta$ of the composites fluctuated slightly but overall exhibited similar $tan\delta$ magnitudes to the respective unfilled polymer particularly at 5 GHz. **Therefore, $SrTiO_3$ based composites can be considered as potential candidates for capacitor materials due to their lower loss tangent and improved permittivity values.** The Lichtenecker and partly the Jayasundere models were in good agreement with the experimental dielectric permitivitty values of the composites. For PBTST and LLDPEST with similar filler loading, the PBT based composites had higher ε' values. $SrTiO_3$ based polymer composites displayed stable dielectric properties over the microwave frequency range.

AUTHORSHIP STATEMENT

All persons who meet authorship criteria are listed as authors, and all authors certify that they have participated sufficiently in the work to take public responsibility for the content, including participation in the concept, design, analysis, writing, or revision of the manuscript.

S. Bahar Baştürk: Conceptualization, Investigation, Methodology, Data curation, Formal analysis, Writing - original draft.

Claire E.J. Dancer: Conceptualization, Data curation, Formal analysis.

Tony McNally: Conceptualization, Investigation, Methodology, Project administration, Supervision, Validation, Writing - review & editing

Declaration of interests

☒ The authors declare that they have no known competing financial interests or personal relationships that could have appeared to influence the work reported in this paper.

Acknowledgements

The authors acknowledge the Scientific and Technological Research Council of Turkey (TÜBİTAK) International Post Doctoral Research Fellowship Programme (BİDEB-2219) who funded this work. Bahar Baştürk thanks the IINM, WMG, University of Warwick for hosting her research visit.

References

1. B. Luo, X. Wang, Y.Wang, L.Li, Fabrication, characterization, properties and theoretical analysis of ceramic/PVDF composite flexible films with high dielectric constant and low dielectric loss, Journal of Materials Chemistry A, 2(2) (2014) 510-519.
2. L. Zhang, J. Zhang, Z.Yue, L.Lı, Thermally stable polymer–ceramic composites for microwave antenna applications, Journal of Advanced Ceramics, 5(4) (2016) 269-276.
3. Zou K., Dan Y., Xu H., Zhang Q., Lu Y., Huang H., He Y, Recent advances in lead-free dielectric materials for energy storage, Materials Research Bulletin, 113, (2019),190-201.
4. Mahmood. A, Naeem. A and Mahmood. T, Chapter 2: High-k Polymer Nanocomposites for Energy Storage Applications, Properties and Applications of Polymer Dielectrics, (2017), Intech Open.
5. Zhang. X, Wen. H, Chen. X, Wu. Y, Xiao. S, Study on the Thermal and Dielectric Properties of $SrTiO_3$/Epoxy Nanocomposites, Energies, 10(5), (2017), 1-14.

6. Alkathy M.S, James Raju K.C, Enhancement of dielectric properties and energy storage density of bismuth and lithium co-substituted strontium titanate ceramics, Ceramics International, 44 (9), (2018), 10367-10375.

7. R.C. Neville, B.Hoenesien, C.A.Mead, Permittivitty of strontium titanate, Journal of Applied Physics, 43, (1972), 2124-2131.

8. Naidu. K.C.B, Sarmash. S, Maddaiah. M, Reddy. P, Rani. D, Subbarao. T, Synthesis and Characterization of MgO-doped $SrTiO_3$ Ceramics, Journal of the Australian Ceramic Society, 52, (2016), 95-101.

9. Yang. H, Fei. Y, Ying. L and Tong. W, Novel Strontium Titanate-Based Lead-Free Ceramics for High-Energy Storage Applications, ACS Sustainable Chem. Eng, 5, (2017), 10215-10222.

10. Zhang. H, Zhu. Y, Li. Z, Fan. P, Ma. W and Xie. B, High discharged energy density of polymer nanocomposites containing paraelectric $SrTiO_3$ nanowires for flexible energy storage device, Journal of Alloys and Compounds, 744, (2018), 116-123.

11. Jimeno. A, Kortaberria. G, Arruti. P, Tercjak. A, Blanco. M and Mondragon. I, Chapter:2 Dynamics and dielectric properties of polymer/nanoparticle nanocomposites by dielectric spectroscopy, Biopolymers and Nanocomposites as Studied by Dielectric Spectroscopy, (2009), Transworld Research Network.

12. Hassan. Y.A and Hu. H, Current status of polymer nanocomposite dielectrics for high-temperature applications, Composites Part A:Applied Science and Manufacturing, 138, 2020, https://doi.org/10.1016/j.compositesa.2020.106064.

13. M.T.Sebastian, H. Jantunen, Polymer-Ceramic Composites of 0-3 connectivity for circuits in electronics: A Review, International Journal of Applied Ceramic Technology, 7(4), (2010), 415-434.

14. Lee. S, Hyun. J.G, Kim. H, Paik. K.W, A study on dielectric constants of epoxy/SrTiO3 composite for embedded capacitor films (ECFs), IEEE Transactions on Advanced Packaging, 30(3), (2007), 428-433.

15. Khutia. M, Joshi. G.M. and Thomas. P, Dielectric relaxation of nano perovskite $SrTiO_3$ reinforced polyester resin/styrene blend for electronic applications, J Mater Sci: Mater Electron, 27, (2016), 7685–7692.

16. Nisa. V.S, Rajesh. S, Murali. K.P, Priyadarsini. V, Potty. S.N. and Ratheesh. R, Preparation, characterization and dielectric properties of temperature stable $SrTiO_3$/PEEK composites for microwave substrate applications, Composites Science and Technology, 68 (1), (2008), 106-112.

17. Rajesh. S, Murali. K.P, Rajani. K.V. and Ratheesh. R, $SrTiO_3$- Filled PTFE Composite Laminates for Microwave Substrate Applications, International Journal of Applied Ceramic Technology, 6, (2009), 553-561.

18. D. Thomas, C. Janardhanan, M.T. Sebastian, Mechanically flexible butyl rubber-$SrTiO_3$ composite dielectrics for microwave applications, International Journal of Applied Ceramic Technology, 8(5), (2011), 1099-1107.

19. F. Xiang, H. Wang, X. Yao, Dielectric properties of SrTiO3/POE flexible composites for microwave applications, Journal of the European Ceramic Society, 27, (2007), 3093-3097.

20. G.S. Deshmukh, D.R. Peshwe, S.U. Pathak, J.D. Ekhe, A study on effect of mineral additions on the mechanical,thermal, and structural properties of poly(butyleneterephthalate) (PBT) composites, Journal of Polymer Research, 18, (2011), 1081-1090.

21. W.Zhou, Thermal and dielectric properties of the AlN particles reinforced linear low-density polyethylene composites, Thermochimica Acta, 512, (2011), 183-188.

22. J. Bian, H.L.Lin, F.X. He, L. Wang, X.W. Wei, I.T. Chang and E. Sancaktar, Processing and assessment of high-performance poly(butylene terephthalate) nanocomposites reinforced with microwave exfoliated graphite oxide nanosheets, European Polymer Journal, 49 (6), (2013), 1406-1423.

23. S. Paszkiewicz, A. Szymczyk, D. Pawlikowska, J. Subocz, M. Zenker, R. Masztak, Electrically and thermally conductive low density polyethylene-based nanocomposites reinforced by MWCNT or hybrid MWCNT/graphene nanoplatelets with improved thermo-oxidative stability, Nanomaterials (Basel), 8(4), (2018), 264.

24. P.S. Grant, C.R.M. Grovenor, Q. Lei, C.E.J. Dancer, Preparation, Microstructure and Microwave dielectric properties of sprayed PFA/barium titanate composite films, Composites Science and Technology, 129, (2016), 198–204.

25. Lu. Z and Yifeng J, Recent progress in dielectric nanocomposites, Materials Science and Technology, 36(1), (2020), 1-16.

26. Xie. T, Wang. Y, Liu. C, Xu. L. New Insights into Sensitization Mechanism of the Doped Ce (IV) into Strontium Titanate, Materials, 11, (2018), 646.

27. Russo. P, Costantini. A, Luciani. G, Tescione. F, Lavorgna. M., Branda, F. and Silvestri. B,. Thermo- mechanical behavior of poly(butylene terephthalate)/silica nanocomposites, Journal of Applied Polymer Science, 135, (2017), 46006.

28. Pereira. G, Cybis. R, Felipe. D, Mazzaferro. L, Forin. D. M, G. M. Oliveira. Mechanical and Thermo-Physical Properties of Short Glass Fiber Reinforced Polybutylene Terephthalate upon Aging in Lubricant/Refrigerant Mixture. Materials Research, 19(6), (2016), 1310-1318.

29. Melissa R. J, F. David H, Sara V.O, Viviana R.C, Kathryn L. B, George H. B, T. Todd. J, Thierry. M.W, Kayla. C.B, Sarah-Jeanne. R, K. David H, Brenda A. J, Jennifer M. Validation of ATR FT-IR to identify polymers of plastic marine debris, including those ingested by marine organisms, Marine Pollution Bulletin, 127, (2018), 704-716.

30. O. Saligheh, M. Forouharshad, R. Arasteh, R. Eslami-Farsani, R. Khajavi, B. Yadollah Roudbari, The effect of multi-walled carbon nanotubes on morphology, crystallinity and mechanical properties of PBT/MWCNT composite nanofibers, Journal of Polymer Research, (2013), 20(65).

31. T.K.B. Sharmila, J.V. Antony, M.P. Jayakrishnan, P.M.S. Beegum, E.T.Thachil, Mechanical, thermal and dielectric properties of hybrid composites of epoxy and reduced graphene oxide/iron oxide, Materials and Design, 90, (2016), 66-75.

32. R.Wang, C. Xie, L. Zeng, H. Xu, Thermal decomposition behavior and kinetics of nanocomposites at low-modified ZnO content, RSC Advances, 9, (2019), 790-800.

33. N. V. Lakshmi, Pankaj Tambe & Niroj Kumar Sahu, Giant permittivity of three phase polymer nanocomposites obtained by modifying hybrid nanofillers with polyvinylpyrrolidone, Composite Interfaces, 25:1, (2018), 47-67.

34. Su. J and Zhang, J, Comparison of rheological, mechanical, electrical properties of HDPE filled with $BaTiO_3$ with different polar surface tension, Applied Surface Science, 388, (2016), 531–538.

35. Ghamdi, F. El-Tantawy, New electromagnetic wave shielding effectiveness at microwave frequency of polyvinyl chloride reinforced graphite/copper nanoparticles, Composites: Part A, 41, (2016), 1693-1701

36. Taya. M, Applications of electronic composites. In Electronic Composites: Modeling, Characterization, Processing, and MEMS Applications, (2005),19-68. Cambridge: Cambridge University Press.

37. M.T. Sebastian, Masurement of microwave dielectric properties and factors affecting them, Dielectric Materials for Wireless Communication, (2008), Elsevier.

38. L. Cadillon Costa, S. Devesa and P. André , Microwave dielectric properties of glass-reinforced polymers, e-Polymers Short Communications 2005, No: 004.

39. A. Dabbak, S.Z. Illias, H.A, B.C. Abdul, N.A. Latiff, M.Z.H. Makmud, Electrical properties of polyethylene/polypropylene compounds for high-voltage insulation, energies, 11, (2018), 1448.

40. J. Topham, O. Boorman, I.L. Hoiser, M. Praeger, R. Torah, A.S. Vaughan, T. Andrritch and S.G. Swingler, Dielectric studies of Polystrene-based high permittivity composite systems, IEEE Conference on Electrical Insulation and Dielectric Phenomena (CEIDP), Des Moines, IA, (2014), 711-714.

41. Tang. H, Lin. Y and Sodano. H.A, Synthesis of High Aspect Ratio $BaTiO_3$ Nanowires for High Energy Density Nanocomposite Capacitors. Adv. Energy Mater, 3, (2013), 451-456.

42. Z. Wang, J.Luo, Zhao. G.L, Dielectric and microwave attenuation properties of graphene nanoplatelet-epoxy composites, AIP Advances, 4, (2014), 017139.

43. Li. L, Zhang. B.Q and Chen. X.M, Dielectric characteristics of PVDF-Polyaniline percolative composites up to microwave frequencies, Applied Physics Letters, 103, (2013), 192902.

44. Chauhan. S. S, Verma. P, Malik. R. S and Choudhary. V, Thermomechanically stable dielectric composites based on poly(ether ketone) and $BaTiO_3$ with improved electromagnetic shielding properties in X- band, J. Appl. Polym. Sci. (2018), 135, 46413.

45. Yang. W, Yu. S, Luo. S, Sun. R, Liao. W.H and Wong. C.P, A systematic study on electrical properties of the $BaTiO_3$-epoxy composite with different sized $BaTiO_3$ as fillers, Journal of Alloys and Compounds, 620, (2015), 315-323.

46. Namitha. L.K and Sebastian. M.T, High permittivity ceramics loaded silicone elastomer composites for flexible electronics applications, Ceramics International, 43 (3), (2017), 2994-3003.

47. Leveque. L, Diaham. S, Valdez-Nava. Z, Laudebat. L and Lebey. T, Effects of filler content on dielectric properties of epoxy/$SrTiO_3$ and epoxy/$BaTiO_3$ composites, Annual Report-Conference on Electrical Insulation and Dielectric Phenomena-CEIDP, art. no. 7352070, 2015, 701-704.

48. Hanemann. T, Gesswein. H, and Schumacher. B, Dielectric property improvement of polymer-nanosized strontium titanate-composites for applications in microelectronics, Microsyst Technol, 17, (2011), 1529-1535.

49. Hao. Y, Wang. X, Bi. K, Zhang. J, Huang. Y, Wu. L, Zhao. P, Xu. K, Lei. M and Li.L, Significantly enhanced energy storage performance promoted by ultimate sized ferroelectric $BaTiO_3$ fillers in nanocomposite films, Nano Energy, 31, (2017), 49-56.

50. Shalu. S, Kar. P, Krupka. J, and Dasgupta. G.B, Synthesis, characterization, thermal, dynamic mechanical, and dielectric studies of $Ba_{0.7}Sr_{0.3}TiO_3$/polystyrene composites, Polym. Compos, 39, (2018), E1714-E1724.

51. G. Subodh, C. Pavithran, P. Mohanan, M.T. Sebastian, PTFE/$Sr_2Ce_2Ti_5O_{16}$ polymer ceramic composites for electronic packaging appliciations, Journal of the European Ceramic Society, 27, (2007), 3039-3044.

52. T. Badapanda, V. Senthil, S. Anwar, L.S. Cavalcante, N.C. Batista, E. Longo, Structural and dielectric properties of polyvinyl alcohol/barium zirconium titanate polymer/ceramic composite, Current Applied Physics, 13, (2013), 1490-1495.

53. K.M. Manu, S. Ananthaumar, M.T. Sebastian, Electrical and thermal properties of low permittivity $Sr_2Al_2SiO_7$ ceramic filled HDPE composites, Ceramics International, 39, (2013), 4945-4951.

54. Q.G. Chi, J.F. Dong, C.H. Zang, C.P. Wong, X. Wang, Q.Q. Lei, Nano iron oxide-deposited calcium copper titanate/polyimide hybrid films induced by an external magnetic field: toward a high dielectric constant and suppressed loss, Journal of Materials Chemistry C, 35, (2016), 8179-8188.

55. F. Qi, N. Chen, Q.Wang, Preparation of PA11/$BaTiO_3$ nanocomposite powders with improved processability, dielectric and piezoelectric properties for use in selective laser sintering, Materials&Design, 131, (2017), 135-143.

56. K. Urano and M. Inoue, Clausius–Mossotti formula for anisotropic dielectrics, J. Chem. Phys. 66, (1977), 791-794.

57. Poon. Y.M, Shin. F.G, A simple explicit formula for the effective dielectric constant of binary 0-3 composites, Journal of Materials Science, 39, (2004),1277–1281.

58. N. Jayasundere and B. V. Smith, Dielectric constant for binary piezoelectric 03 composites, Journal of Applied Physics 73,(1993), 2462-2466.

59. Goncharenko. A.V, Lozovski. V. Z, and Venger. E. F, Lichtenecker's equation: applicability and limitations. Optics Communications, 174(1–4), (2000), 19–32.